

# Dithienopyrrole Based Small Molecule with Low Band Gap for Organic Solar Cells

Miaomiao Li, Wang Ni, Huanran Feng, Bin Kan, Xiangjian Wan,\*  
Yamin Zhang, Xuan Yang, and Yongsheng Chen\*

*Key Laboratory for Functional Polymer Materials, Centre for Nanoscale Science and Technology,  
Institute of Polymer Chemistry, Collaborative Innovation of Chemical Science and Engineering (Tianjin),  
College of Chemistry, Nankai University, Tianjin 300071, China*

A low band gap acceptor-donor-acceptor (A-D-A) small molecule donor material, named DR3TDTN, has been designed and synthesized for solution-processed organic solar cells. DR3TDTN shows narrow optical band gap with value of 1.49 eV and broad absorption spectrum from 300 to 820 nm. The HOMO and LUMO energy levels of DR3TDTN are -4.74 and -3.26 eV, respectively. The optimized photovoltaic device based on DR3TDTN:PC<sub>71</sub>BM blend film shows a power conversion efficiency of 3.03% with an open-circuit voltage of 0.67 V, a short-circuit current of 8.22 mA•cm<sup>-2</sup> and fill factor of 0.55.

**Keywords** organic solar cells, low band gap, small molecule, HOMO energy level

## Introduction

Solution-processed organic photovoltaic cells (OPVs) have been studied intensively in the past few years due to the advantages of light-weight, low cost and the potential to fabricate flexible devices.<sup>[1-8]</sup> Many efforts have been focused on polymer-based OPVs<sup>[9-18]</sup> and power conversion efficiencies (PCEs) around 10% have been achieved.<sup>[19-23]</sup> Compared to polymer materials, small molecules show competitive advantages, such as definite molecule structure and therefore less batch-to-batch variation, easier band structure control, etc.<sup>[24-31]</sup> To date, solution-processed small molecule based OPVs have achieved PCEs over 9% through design and synthesis of new small molecule materials and optimization of device fabrication.<sup>[32-34]</sup>

The PCE of OPVs is determined by the three parameters open-circuit voltage ( $V_{oc}$ ), short-circuit current ( $J_{sc}$ ) and fill factor (FF). Recently, small molecule based OPVs with high  $V_{oc}$  over 0.9 V and high FF over 0.70 have been reported by several groups.<sup>[34-36]</sup> However, the  $J_{sc}$  of small molecule based OPVs is still far behind polymer based OPVs. The  $J_{sc}$  is mainly limited by the light absorption which depends on the band gap of small molecule donor materials. Therefore, to achieve high  $J_{sc}$ , design and synthesis of new donor materials with narrow band gap are in high demand. The band gap is determined by the difference of the highest occupied molecular orbital (HOMO) energy level and the lowest unoccupied molecular orbital (LUMO) energy level of

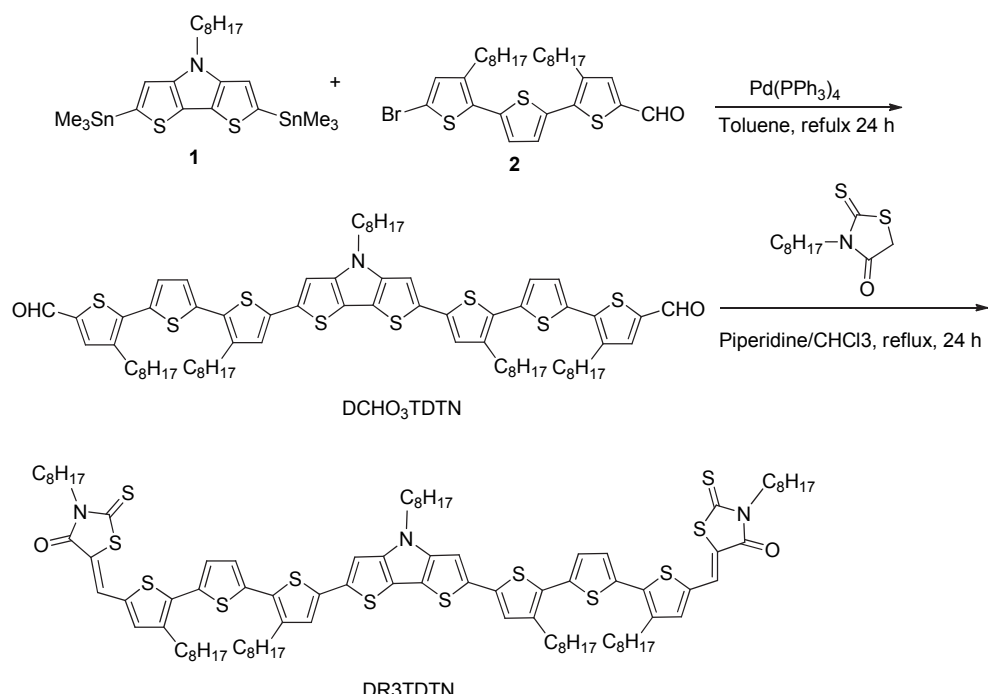
the donor material. For acceptor-donor-acceptor (A-D-A) type small molecules, the HOMO energy levels mainly depend on the central donor segments, and the LUMO energy levels depend on the terminal acceptor units.<sup>[37-39]</sup> Thus, introducing stronger electron-donating central units to enhance the HOMO energy levels, or stronger electron-withdrawing terminal acceptors to lower the LUMO levels could be an efficient way to reduce the band gap and to extend the absorption band of A-D-A molecules. It is to be noted that low  $V_{oc}$  might be an adverse effect due to the enhanced HOMO. However, it is expected that a balance between the  $J_{sc}$  and  $V_{oc}$ , and high  $J_{sc}$  could be obtained through molecules design and device optimization. In our recent works, we have synthesized a series of linear A-D-A small molecules with benzodithiophene (BDT) as the central donor unit and alkyl-rhodanine as the terminal acceptor unit (Scheme 1).<sup>[40-42]</sup> These molecules showed absorption onset around 700 nm with relatively wide band gaps (*ca.* 1.75 eV).

In this work, using the above strategy for designing low band small molecule, herein, we have chosen dithienopyrrole, an efficient electron donating unit widely used in organic optoelectronic materials<sup>[27,43-45]</sup> as the central building unit to design and synthesize a new A-D-A molecule, named DR3TDTN (Scheme 1) with dithienopyrrole as the core, octyl-rhodanine as the terminal acceptor, and terthiophene as the  $\pi$ -bridge. The new molecule, with strong electron-donating dithieno-

\* E-mail: xjwan@nankai.edu.cn, yschen99@nankai.edu.cn; Fax: 0086-022-23499992

Received March 2, 2015; accepted April 2, 2015; published online May 5, 2015.

Supporting information for this article is available on the WWW under <http://dx.doi.org/10.1002/cjoc.201500170> or from the author.

**Scheme 1** Synthesis routes of DR3TDTN

pyrrole as the donor unit, indeed obtains much lower optical band gap with value of 1.49 eV, and a broad absorption band from 300 to 830 nm. The photovoltaic device based on DR3TDTN:PC<sub>71</sub>BM blend film shows a PCE of 3.03% with a  $V_{oc}$  of 0.67 V, a  $J_{sc}$  of 8.22 mA•cm<sup>-2</sup> and FF of 0.55.

## Experimental

### General experimental section

All reactions and manipulations were carried out under argon atmosphere using standard Schlenk techniques. All starting materials were purchased from commercial suppliers and used without further purification.

### Synthesis procedures

2,6-Bis(tri-methyl)-N-(octyl)-dithieno[3,2-b:2',3'-d]pyrrole (**1**) and 5-bromo-3,3-di-octyl-2,2':5,2''-terthiophene-2-carbaldehyde (**2**) were synthesized according to the literatures.<sup>[45,46]</sup>

A solution of **1** (1.46 g, 2.36 mmol) and **2** (3.28 g, 5.66 mmol) in dry toluene (50 mL) was degassed twice with argon followed by the addition of Pd(PPh<sub>3</sub>)<sub>4</sub> (40 mg, 0.035 mmol). After stirring at 110 °C for 24 h under argon, the mixture was poured into water (200 mL), and extracted with chloroform. The organic layer was washed with water, and then dried over Na<sub>2</sub>SO<sub>4</sub>, and evaporated. The residue was purified by silica gel chromatography using a mixture of petroleum ether and dichloromethane ( $V:V=1:2$ ) as eluant to afford compound DCHO<sub>3</sub>TDTN (1.82 g, 60%). <sup>1</sup>H NMR (400 MHz, CDCl<sub>3</sub>) δ: 9.79 (s, 2H), 7.56 (s, 2H), 7.25–6.90 (b, 8H), 4.14–4.02 (m, 2H), 2.90–2.64 (m, 8H),

1.90–1.80 (m, 2H), 1.70–1.60 (m, 8H), 1.48–1.20 (m, 50H), 0.94–0.82 (m, 15H); MS (MALDI-TOF)  $m/z$ : 1287.49 [M<sup>+</sup>]. Anal. calcd for C<sub>74</sub>H<sub>97</sub>NO<sub>2</sub>S<sub>8</sub>: C 68.95, H 7.58, N 1.09; found C 68.71, H 7.51, N 1.16.

### Synthesis of DR3TDTN

To a chloroform (50 mL) solution of DCHO<sub>3</sub>TDTN (0.30 g, 0.208 mmol), octyl-rhodanine (0.60 g, 2.44 mmol) and three drops of piperidine were added. The resulting solution was refluxed for 24 h under argon. Then, the mixture was poured into water (200 mL), and extracted with chloroform. The organic layer was washed with water, and then dried over anhydrous Na<sub>2</sub>SO<sub>4</sub>. The solvent was removed under reduced pressure. The residue was purified by silica gel chromatography using a mixture of chloroform and petroleum ( $V:V=3:1$ ) as eluant, and the crude solid was recrystallized using hexane and chloroform to afford DR3TDTN (0.26 g, 64%). <sup>1</sup>H NMR (400 MHz, CDCl<sub>3</sub>) δ: 7.73 (s, 2H), 7.20–6.90 (b, 10H), 4.20–4.02 (m, 6H), 2.94–2.64 (m, 8H), 1.96–1.80 (m, 2H), 1.78–1.64 (m, 12H), 1.35–1.20 (m, 70H), 0.98–0.86 (m, 21H); MS (MALDI-TOF)  $m/z$ : 1741.67 [M<sup>+</sup>]. Anal. calcd for C<sub>96</sub>H<sub>131</sub>N<sub>3</sub>O<sub>2</sub>S<sub>12</sub>: C 66.12, H 7.57, N 2.41; found C 66.16, H 7.99, N 2.58.

### Measurements and instruments

The H<sup>1</sup> NMR spectra were taken on a Bruker AV400 Spectrometer. Matrix assisted laser desorption/ionization time-of-flight (MALDI-TOF) mass spectra were performed on a Bruker Autoflex III instrument. The thermogravimetric analyses (TGA) were carried out on a NETZSCH STA 409PC instrument under purified nitrogen gas flow with a 10 °C•min<sup>-1</sup> heating rate.

UV-vis spectra were obtained with a JASCO V-570 spectrophotometer. X-ray diffraction (XRD) experiments were performed on a Bruker D8 FOCUS X-ray diffractometer with Cu K $\alpha$  radiation ( $\lambda=1.5406\text{ \AA}$ ) at a generator voltage of 40 kV and a current of 40 mA. Atomic force microscope (AFM) investigation was performed using Bruker MultiMode 8 in “tapping” mode. Cyclic voltammetry (CV) experiments were performed with a LK98B II Microcomputer-based Electrochemical Analyzer in dichloromethane solutions. All CV measurements were carried out at room temperature with a conventional three-electrode configuration employing a glassy carbon electrode as the working electrode, a saturated calomel electrode (SCE) as the reference electrode, and a Pt wire as the counter electrode. Dichloromethane was distilled from calcium hydride under dry argon immediately prior to use. Tetrabutylammonium phosphorus hexafluoride ( $\text{Bu}_4\text{NPF}_6$ , 0.1 mol·L $^{-1}$ ) in dichloromethane was used as the supporting electrolyte, and the scan rate was 100 mV·s $^{-1}$ . Hole mobility was measured by space charge limited current (SCLC) method using a diode configuration of ITO/PEDOT:PSS/donor:PC $_7$ BM/Au by taking the dark current density in the range of 0–6 V and fitting the results to a space charge limited form, where SCLC is described by:

$$J = \frac{9\varepsilon_0\varepsilon_r\mu_0 V^2}{8L^3} \exp(0.89\beta\sqrt{\frac{V}{L}})$$

where  $J$  is the current density,  $L$  is the film thickness of the active layer,  $\mu_0$  is the hole mobility,  $\varepsilon_r$  is the relative dielectric constant of the transport medium,  $\varepsilon_0$  is the permittivity of free space ( $8.85 \times 10^{-12}\text{ F}\cdot\text{m}^{-1}$ ),  $V$  ( $V_{\text{appl}} - V_{\text{bi}}$ ) is the internal voltage of the device,  $V_{\text{appl}}$  is the applied voltage to the device and  $V_{\text{bi}}$  is the built-in voltage due to the relative work function difference of the two electrodes.

The current density-voltage ( $J$ - $V$ ) characteristics of photovoltaic devices were obtained by a Keithley 2400 source-measure unit. The photocurrent was measured under illumination simulated 100 mW·cm $^{-2}$  AM1.5G irradiation using a xenon-lamp-based solar simulator [Oriel 96000 (AM1.5G)] in an argon filled glove box. Simulator irradiance was characterized using a calibrated spectrometer and illumination intensity was set using a certified silicon diode. External quantum efficiency (EQE) value of the encapsulated device was obtained with a halogen-tungsten lamp, monochromator, optical chopper, and lock-in amplifier in air and photon flux was determined by a calibrated silicon photodiode.

### Fabrication of organic solar cells

The photovoltaic devices were fabricated with a structure of glass/ITO/PEDOT:PSS/donor:acceptor/ZnO/Al. The ITO-coated glass substrates were cleaned subsequently by ultrasonic treatment in detergent, deionized water, acetone, and isopropyl alcohol under ultrasonication for 15 min each solvent and then dried

by a nitrogen flow. A thin layer of PEDOT:PSS (Baytron P VP AI 4083, filtered at 0.45  $\mu\text{m}$ ) was spin-coated (3000 r/min, ca. 40 nm thick) onto ITO surface. After being baked at 150 °C for 20 min, the substrates were transferred into an argon-filled glove box. Then, the active layer was spin-coated from donor (10 mg/mL):PC $_7$ BM blend chloroform solution with different ratios at 1700 r/min for 20 s. Subsequently, ZnO particle suspension was used to spin-coat the ZnO layer on top of the active layers.<sup>[47]</sup> Thermal annealing was carried out on a digitally controlled hotplate at various temperatures after ZnO spin coating in an argon-filled glove box. Finally, 50 nm Al layer was deposited on ZnO film under high vacuum ( $<2 \times 10^{-4}\text{ Pa}$ ). The thickness of active layers was measured using Dektak 150 profilometer. The effective area of each cell was 4 mm $^2$  defined by masks for the solar cell devices discussed in this work.

## Results and Discussion

### Thermal and optical property

As shown in Figure 1a, molecule DR3TDTN exhibits good thermal stability with 5% weight-loss temperature at 360 °C under N $_2$  atmosphere. The UV-Vis absorption spectra of DR3TDTN in chloroform solution and in the thin film are shown in Figure 1b, and some important optical data are summarized in Table 1. As shown in Figure 1b, DR3TDTN in chloroform

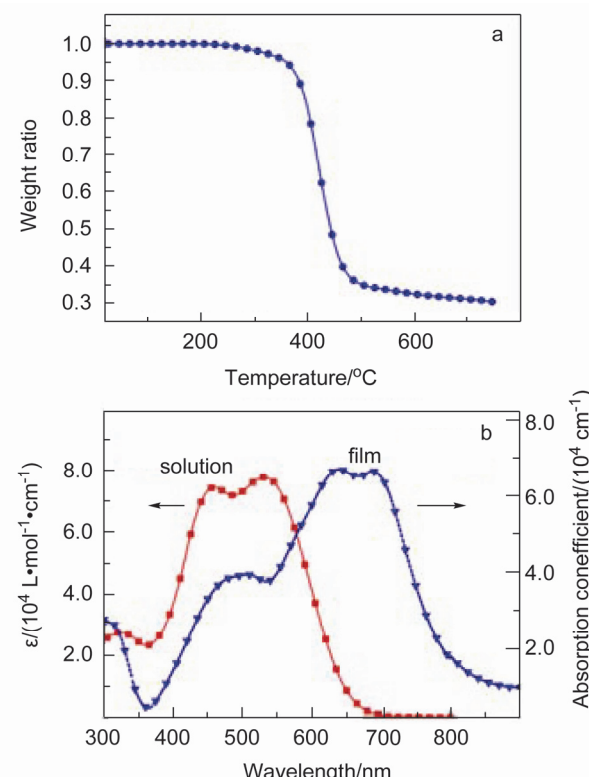


**Figure 1** (a) TGA curves of DR3TDTN with a heating rate of 10 °C/min under N $_2$  atmosphere and (b) absorption spectra of DR3TDTN in chloroform solution and in as-cast film.

( $10^{-6}$  mol·L $^{-1}$ ) shows an absorption peak at 532 nm with a maximum absorption coefficient of  $7.8 \times 10^4$  L·mol $^{-1} \cdot \text{cm}^{-1}$ . The DR3TDTN film cast from chloroform shows a red-shifted maximum absorption peak at 638 nm, and broad absorption band from 350 to 820 nm. In addition, the DR3TDTN film shows a vibronic shoulder peak at 688 nm, indicating effective  $\pi$ - $\pi$  packing between the molecule backbones. The optical band gap of DR3TDTN is 1.49 eV estimated from the onset of the film absorption spectrum.

**Table 1** Optical and electrochemical data of DR3TDTN

$\lambda_{\max}^{\text{sol}} / \text{nm}$	$\epsilon^{\text{sol}} / (\text{L} \cdot \text{mol}^{-1} \cdot \text{cm}^{-1})$	$\lambda_{\max}^{\text{film}} / \text{nm}$	$E^{\text{opt}}_{\text{g}} / \text{eV}$	HOMO/eV	LUMO/eV
532	$8.2 \times 10^4$	638	1.49	-4.74	-3.26

### Electrochemical properties

The electrochemical properties of DR3TDTN was investigated by cyclic voltammogram with ferrocene/ferrocenium of the ( $\text{Fc}/\text{Fc}^+$ ) redox couple (4.8 eV below the vacuum level) as the internal calibration. The HOMO and LUMO energy levels of DR3TDTN are estimated based on the onset oxidation potential and the onset reduction potential of the redox curve as shown in Figure 2, which are -4.74 and -3.26 eV, respectively. Compared with our previous A-D-A molecules with BDT as the core,<sup>[31,38]</sup> the new small molecule with dithienopyrrole as the central building block indeed shows an increased HOMO energy level, which also demonstrates that the HOMO energy level of the A-D-A small molecule indeed can be fine tuned by changing the central donor unit. The electrochemical band gap of DR3TDTN is 1.48 eV, which is consistent with the value of optical band gap. The narrow band gap of DR3TDTN is attributed to the increased HOMO energy level.

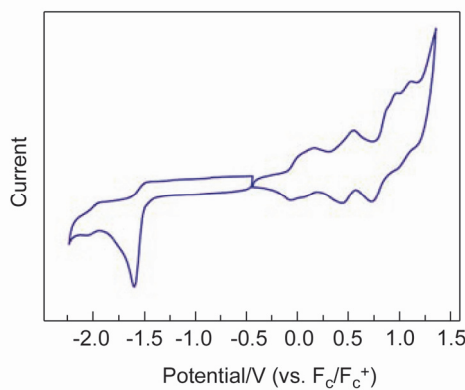


**Figure 2** Cyclic voltammogram of DR3TDTN in a dichloromethane solution of  $0.1 \text{ mol} \cdot \text{L}^{-1}$   $\text{Bu}_4\text{NPF}_6$  with a scan rate of  $100 \text{ mV} \cdot \text{s}^{-1}$ .

### Photovoltaic properties

Bulk heterojunction organic solar cells were fabricated using DR3TDTN as the electron donor material

and PC<sub>71</sub>BM as the electron acceptor material with a device structure of glass/ITO/PEDOT:PSS/DR3TDTN:PC<sub>71</sub>BM/ZnO/Al, using the conventional solution spin-coating process. The corresponding parameters of device performance are summarized in Table 2. The current density vs. voltage ( $J-V$ ) curves measured under AM 1.5G illumination at an intensity of  $100 \text{ mW} \cdot \text{cm}^{-2}$  are shown in Figure 3a. Device optimization was conducted by varying the weight ratios of donor/acceptor. The best result is observed for a donor/acceptor weight ratio of 1 : 0.8 from chloroform solution. For DR3TDTN without any post treatment, a low PCE of 0.67% is obtained with a  $V_{\text{oc}}$  of 0.69 V, a  $J_{\text{sc}}$  of  $2.95 \text{ mA} \cdot \text{cm}^{-2}$  and a FF of 0.33. Further improvement of the PCE was achieved by gradient heating process. The photovoltaic performances of the devices with thermal annealing at different temperatures are shown in Table S1. After  $120^\circ\text{C}$  thermal annealing for 10 min, the PCEs increase to 3.03% for DR3TDTN, which is attributed to increase of both  $J_{\text{sc}}$  and FF as shown in Table 2. EQE spectrum of the optimized OPV device based on DR3TDTN is shown in Figure 3b. From EQE spectrum, it is apparent that DR3TDTN-based device exhibits broad photo-to-current response from 300 to about 800 nm, but the highest EQE value is only 35%. The relatively low EQE response of DR3TDTN results in the relatively low  $J_{\text{sc}}$ , which is attributed to the poor morphology of blend film, as discussed below.

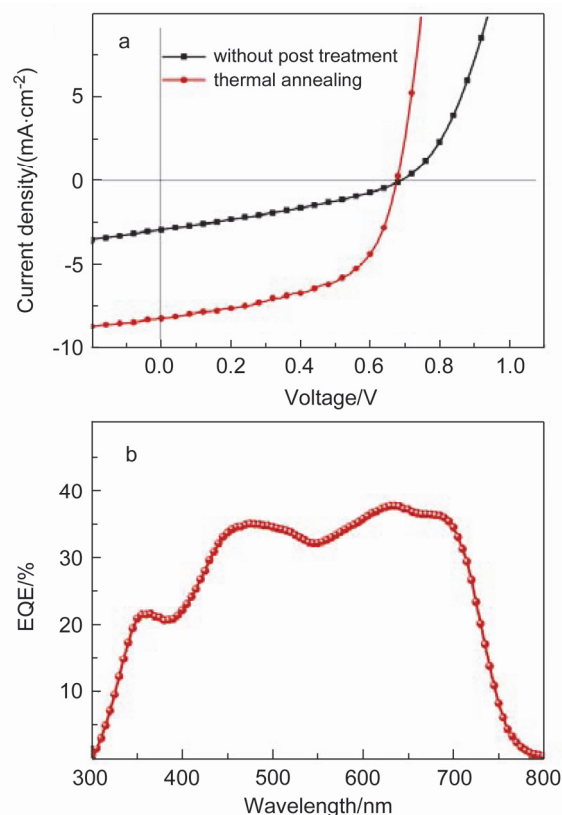


**Figure 3** (a)  $J-V$  curves of the devices based on DR3TDTN:PC<sub>71</sub>BM (1 : 0.8,  $w:w$ ) and (b) EQE of the optimized device based on DR3TDTN:PC<sub>71</sub>BM (1 : 0.8,  $w:w$ ).

**Table 2** Device performance parameters of the organic solar cells based on DR3TDTN:PC<sub>71</sub>BM blend films with different treatment

Donor : acceptor	$V_{oc}/V$	$J_{sc}/(\text{mA} \cdot \text{cm}^{-2})$	FF	PCE (PCE <sub>ave</sub> <sup>b</sup> )/%
1 : 0.5	0.70	2.22	0.33	0.52 (0.46)
1 : 0.5 <sup>a</sup>	0.68	7.12	0.52	2.52 (2.37)
1 : 0.8	0.69	2.95	0.33	0.67 (0.62)
1 : 0.8 <sup>a</sup>	0.67	8.22	0.55	3.03 (2.90)
1 : 1	0.69	2.40	0.32	0.53 (0.48)
1 : 1 <sup>a</sup>	0.67	7.43	0.54	2.69 (2.53)

<sup>a</sup> Annealing at 120 °C for 10 min. <sup>b</sup> Average over 20 devices.

### XRD and morphology analysis

The packing properties of DR3TDTN were investigated by the XRD analyses of pure DR3TDTN films without and with thermal annealing. As shown in Figure 4, DR3TDTN film as casted from chloroform exhibits a strong diffraction peak (100) at  $2\theta=4.69^\circ$  demonstrating good molecule stacking in the film spin-coated from chloroform. After thermal annealing at 120 °C for 10 min, a significantly increased intensity (100) diffraction peak at  $2\theta=4.719^\circ$  and a second-order diffraction peak at  $2\theta=9.38^\circ$  are observed, indicating that more organized assembly and higher crystallinity of DR3TDTN are produced after thermal annealing. The XRD results of DR3TDTN films indicate that thermal annealing leads to the better molecular packing, which would be of benefit for charge transport. As plotted in Figure 5, the hole mobilities of the DR3TDTN:PC<sub>71</sub>BM blend films through the hole-only devices were measured using the space charge limited current (SCLC) method. The mobility increased from  $7.61 \times 10^{-5}$  to  $2.86 \times 10^{-4} \text{ cm}^2 \cdot \text{V}^{-1} \cdot \text{s}^{-1}$  for blend films before and after 120 °C thermal annealing, which is ascribed to the better molecular packing after thermal annealing.

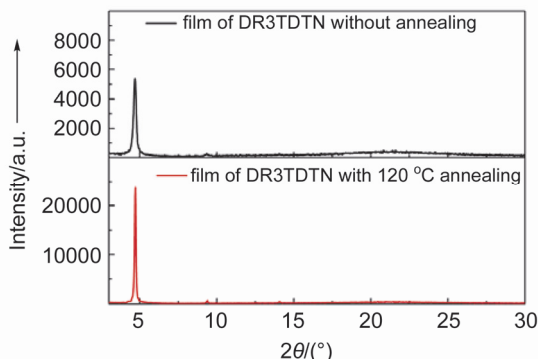


**Figure 4** XRD patterns of DR3TDTN films spin-coated from chloroform onto glass substrates.

The morphologies of DR3TDTN:PC<sub>71</sub>BM blend films were investigated by AFM. As shown in Figure 6, root mean square (rms) roughness of DR3TDTN:PC<sub>71</sub>BM blend film without any post treatment is 0.324 nm. And the film shows no obvious phase separation of the donor and the acceptor. After 120 °C thermal

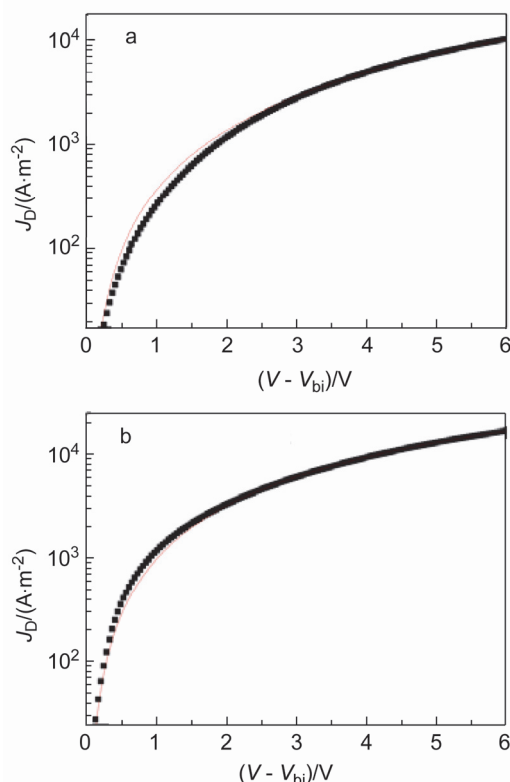


**Figure 5**  $J$ - $V$  characteristics of hole-only devices with a configuration of ITO/PEDOT:PSS (30 nm)/DR3TDTN:PC<sub>71</sub>BM / Au (30 nm). (a) without post treatment; (b) with 120 °C thermal annealing.

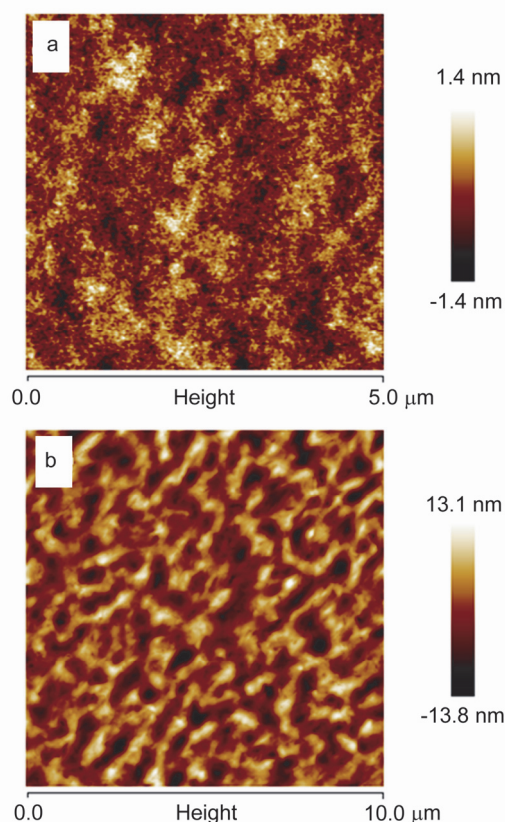


**Figure 6** The AFM images of DR3TDTN:PC<sub>71</sub>BM blend films. (a) without post treatment; (b) with 120 °C thermal annealing.

annealing, the roughness of DR3TDTN:PC<sub>71</sub>BM blend film increases to 3.24 nm, which could be caused by the increased packing and aggregation of DR3TDTN.<sup>[48,49]</sup> The results are consistent with the XRD data of DR3TDTN. Moreover, the DR3TDTN:PC<sub>71</sub>BM blend film with annealing exhibits obvious phase separation and interpenetrating network morphology, which benefit charge transport, thus leading to increased  $J_{sc}$ . However, the well packing property of DR3TDTN leads to large domains with size of *ca.* 200 nm in the blend film, which is much larger than the ideal exciton diffusion length (10–20 nm).<sup>[50,51]</sup> The large domains will cause serious charge recombination, thus inferior FF and low EQE response. In comparison with some high efficiency benzo[1,2-b:4,5-b'] dithiophene (BDT) based donor molecules we have reported,<sup>[41,46]</sup> the low photovoltaic performance of DR3TDTN based device is mainly due to its inferior morphology in the active layer with large domains (*ca.* 200 nm for DR3TDTN blend and *ca.* 20 nm for those BDT based molecules bended with PC<sub>71</sub>BM). Higher device performance is expected if small domains around 20 nm can be obtained through further device optimization.

## Conclusions

In this work, we designed and synthesized a new A-D-A small molecule donor material, DR3TDTN, with dithienopyrrole as the core, and octyl-rhodanine as the terminal acceptor. The molecule shows high HOMO level of –4.74 eV, and broad absorption from 300 to 820 nm with a narrow optical band gap of 1.49 eV. The optimized photovoltaic device based on DR3TDTN:PC<sub>71</sub>BM blend film shows a PCE of 3.03% with a  $V_{oc}$  of 0.67 V, a  $J_{sc}$  of 8.22 mA•cm<sup>–2</sup> and FF of 0.55. The relatively low  $J_{sc}$  and FF could be attributed to the poor morphology of the active layer. It is believed that the OPV performance of the devices based on DR3TDTN could be much enhanced through controlling and optimizing the morphology of DR3TDTN:PC<sub>71</sub>BM blend films. Furthermore, our results demonstrate that the introduction of strong electron-donating dithienopyrrole as the core could be an efficient way to enhance HOMO energy level and thus to achieve narrow band gap for A-D-A small molecule donor materials.

## Acknowledgement

The authors gratefully acknowledge the financial support from MoST (No. 2014CB643502), the National Natural Science Foundation of China (Nos. 91433101, 51373078 and 51422304) and the Natural Science Foundation of Tianjin City (No. 13RCGFGX01121).

## References

- [1] Heeger, A. J. *Chem. Soc. Rev.* **2010**, *39*, 2354.
- [2] Roncali, J. *Acc. Chem. Res.* **2009**, *42*, 1719.
- [3] Zhou, H. X.; Yang, L. Q.; You, W. *Macromolecules* **2012**, *45*, 607.
- [4] Ye, L.; Zhang, S. Q.; Huo, L. J.; Zhang, M. J.; Hou, J. H. *Acc. Chem. Res.* **2014**, *47*, 1595.
- [5] Zhang, J.; Cai, W. Z.; Huang, F.; Wang, E. G.; Zhong, C. M.; Liu, S. J.; Wang, M.; Duan, C. H.; Yang, T. B.; Cao, Y. *Macromolecules* **2011**, *44*, 894.
- [6] Li, Y. F. *Acc. Chem. Res.* **2012**, *45*, 723.
- [7] Krebs, F. C. *Sol. Energy Mater. Sol. Cells* **2009**, *93*, 394.
- [8] Scharber, M. C.; Mühlbacher, D.; Koppe, M.; Denk, P.; Waldauf, C.; Heeger, A. J.; Brabec, C. J. *Adv. Mater.* **2006**, *18*, 789.
- [9] Wang, J. T.; Ye, H. Y.; Li, H. J.; Mei, C. Y.; Ling, J.; Li, W. S.; Shen, Z. Q. *Chin. J. Chem.* **2013**, *31*, 1367.
- [10] Zhou, H. X.; Yang, L. Q.; Stuart, A. C.; Price, S. C.; Liu, S. B.; You, W. *Angew. Chem., Int. Ed.* **2011**, *50*, 2995.
- [11] Chen, L.; Shen, X. X.; Chen, Y. W. *Chin. J. Chem.* **2012**, *30*, 2219.
- [12] Min, J.; Zhang, Z. G.; Zhang, S. Y.; Li, Y. F. *Chem. Mater.* **2012**, *24*, 3247.
- [13] Qu, S. Y.; Tian, H. *Chem. Commun.* **2012**, *48*, 3039.
- [14] Huang, L. Q.; Yang, D.; Gao, Q.; Liu, Y.; Lu, S. M.; Zhang, J.; Li, C. *Chin. J. Chem.* **2013**, *31*, 1385.
- [15] Cao, W. R.; Xue, J. G. *Energy Environ. Sci.* **2014**, *7*, 2123.
- [16] Chen, J. W.; Cao, Y. *Acc. Chem. Res.* **2009**, *42*, 1709.
- [17] Deng, Y. F.; Liu, J.; Wang, J. T.; Liu, L. H.; Li, W. L.; Tian, H. K.; Zhang, X. J.; Xie, Z. Y.; Geng, Y. H.; Wang, F. S. *Adv. Mater.* **2014**, *26*, 471.
- [18] Yan, Q. X.; Zuo, L. J.; Gu, Z. W.; Yang, L. G.; Wang, R.; Wang, M.; Chen, H. Z. *Chin. J. Chem.* **2013**, *31*, 1380.
- [19] He, Z. C.; Zhong, C. M.; Su, S. J.; Xu, M.; Wu, H. B.; Cao, Y. *Nat. Photonics* **2012**, *6*, 591.
- [20] Chen, J. D.; Cui, C. H.; Li, Y. Q.; Zhou, L.; Ou, Q. D.; Li, C.; Li, Y. F.; Tang, J. X. *Adv. Mater.* **2015**, *27*, 1035.
- [21] Zhang, W. J.; Wu, Y. L.; Bao, Q. Y.; Gao, F.; Fang, J. F. *Adv. Energy Mater.* **2014**, *4*, 1400359.
- [22] Guo, X.; Zhang, M. J.; Ma, W.; Ye, L.; Zhang, S. Q.; Liu, S. J.; Ade, H.; Huang, F.; Hou, J. H. *Adv. Mater.* **2014**, *26*, 4043.
- [23] Zhang, S. Q.; Ye, L.; Zhao, W. C.; Yang, B.; Wang, Q.; Hou, J. *Sci. Chin. Chem.* **2015**, *58*, 248.
- [24] Shen, S. L.; Jiang, P.; He, C.; Zhang, J.; Shen, P.; Zhang, Y.; Yi, Y. P.; Zhang, Z. J.; Li, Z. B.; Li, Y. F. *Chem. Mater.* **2013**, *25*, 2274.
- [25] Lin, Y. Z.; Li, Y. F.; Zhan, X. W. *Chem. Soc. Rev.* **2012**, *41*, 4245.
- [26] Walker, B.; Kim, C.; Nguyen, T.-Q. *Chem. Mater.* **2010**, *23*, 470.
- [27] Wessendorf, C. D.; Schulz, G. L.; Mishra, A.; Kar, P.; Ata, I.; Weideler, M.; Urdanpilleta, M.; Hanisch, J.; Mena-Osteritz, E.; Lindén, M.; Ahlsweide, E.; Bäuerle, P. *Adv. Energy Mater.* **2014**, *4*, 00266.
- [28] Deng, D.; Zhang, Y. J.; Yuan, L.; He, C.; Lu, K.; Wei, Z. X. *Adv. Energy Mater.* **2014**, *00538*.
- [29] Huang, J. H.; Zhan, C. L.; Zhang, X.; Zhao, Y.; Lu, Z. H.; Jia, H.; Jiang, B.; Ye, J.; Zhang, S. L.; Tang, A. L.; Liu, Y. Q.; Pei, Q. B.; Yao, J. N. *ACS Appl. Mater. Inter.* **2013**, *5*, 2033.
- [30] Li, C.; Chen, Y. J.; Zhao, Y.; Wang, H. F.; Zhang, W.; Li, Y. W.; Yang, X. M.; Ma, C. Q.; Chen, L. W.; Zhu, X. L.; Tu, Y. F. *Nanoscale* **2013**, *5*, 9536.
- [31] Bobe, S. R.; Gupta, A.; Ranjanaware, A.; Bilic, A.; Bhosale, S. V.; Bhosale, S. V. *RSC Adv.* **2015**, *5*, 4411.
- [32] Kyaw, A. K. K.; Wang, D. H.; Wynands, D.; Zhang, J.; Nguyen, T.-Q.; Bazan, G. C.; Heeger, A. J. *Nano Lett.* **2013**, *13*, 3796.
- [33] Zhang, Q.; Kan, B.; Liu, F.; Long, G. K.; Wan, X. J.; Chen, X. Q.; Zuo, Y.; Ni, W.; Zhang, H. J.; Li, M. M.; Hu, Z. C.; Huang, F.; Cao, Y.; Liang, Z. Q.; Zhang, M. T.; Russell, T. P.; Chen, Y. S. *Nat. Photonics* **2015**, *9*, 35.
- [34] Kan, B.; Zhang, Q.; Li, M. M.; Wan, X. J.; Ni, W.; Long, G. K.; Wang, Y. C.; Yang, X.; Feng, H. R.; Chen, Y. S. *J. Am. Chem. Soc.* **2014**, *136*, 15529.
- [35] Lin, Y. Z.; Ma, L. C.; Li, Y. F.; Liu, Y. Q.; Zhu, D. B.; Zhan, X. W. *Adv. Energy Mater.* **2014**, *4*, 00626.

- [36] Du, Z. K.; Chen, W. C.; Chen, Y. H.; Qiao, S. L.; Bao, X. C.; Wen, S. G.; Sun, M. L.; Han, L. L.; Yang, R. Q. *J. Mater. Chem. A* **2014**, *2*, 15904.
- [37] Ni, W.; Li, M. M.; Kan, B.; Zuo, Y.; Zhang, Q.; Long, G. K.; Feng, H. R.; Wan, X. J.; Chen, Y. S. *Org. Electron.* **2014**, *15*, 2285.
- [38] He, G. R.; Li, Z.; Wan, X. J.; Zhou, J. Y.; Long, G. K.; Zhang, S. Z.; Zhang, M. T.; Chen, Y. S. *J. Mater. Chem. A* **2013**, *1*, 1801.
- [39] Chen, Y. S.; Wan, X. J.; Long, G. K. *Acc. Chem. Res.* **2013**, *46*, 2645.
- [40] Ni, W.; Li, M. M.; Wan, X. J.; Feng, H. R.; Kan, B.; Zuo, Y.; Chen, Y. S. *RSC Adv.* **2014**, *4*, 31977.
- [41] Zhou, J. Y.; Zuo, Y.; Wan, X. J.; Long, G. K.; Zhang, Q.; Ni, W.; Liu, Y. S.; Li, Z.; He, G. R.; Li, C. X.; Kan, B.; Li, M. M.; Chen, Y. S. *J. Am. Chem. Soc.* **2013**, *135*, 8484.
- [42] Liu, Y. S.; Wan, X. J.; Wang, F.; Zhou, J. Y.; Long, G. K.; Tian, J. G.; Chen, Y. S. *Adv. Mater.* **2011**, *23*, 5387.
- [43] Zhan, X. W.; Tan, Z. A.; Zhou, E. J.; Li, Y. F.; Misra, R.; Grant, A.; Domercq, B.; Zhang, X. H.; An, Z. S.; Zhang, X.; Barlow, S.; Kippelen, B.; Marder, S. R. *J. Mater. Chem.* **2009**, *19*, 5794.
- [44] Zhang, X.; Steckler, T. T.; Dasari, R. R.; Ohira, S.; Potsavage, W.; J.; Tiwari, S. P.; Coppee, S.; Ellinger, S.; Barlow, S.; Bredas, J.-L.; Kippelen, B.; Reynolds, J. R.; Marder, S. R. *J. Mater. Chem.* **2010**, *20*, 123.
- [45] Evenson, S. J.; Pappenfus, T. M.; Delgado, M. C. R.; Radke-Wohlers, K. R.; Navarrete, J. T. L.; Rasmussen, S. C. *Phys. Chem. Chem. Phys.* **2012**, *14*, 6101.
- [46] Zhou, J. Y.; Wan, X. J.; Liu, Y. S.; Zuo, Y.; Li, Z.; He, G. R.; Long, G. K.; Ni, W.; Li, C. X.; Su, X. C.; Chen, Y. S. *J. Am. Chem. Soc.* **2012**, *134*, 16345.
- [47] Beek, W. J. E.; Wienk, M. M.; Kemerink, M.; Yang, X. N.; Janssen, R. A. J. *J. Phys. Chem. B* **2005**, *109*, 9505.
- [48] Wang, Y. F.; Bai, H. T.; Cheng, P.; Zhang, M. Y.; Zhan, X. W. *Sci. Chin. Chem.* **2015**, *58*, 331.
- [49] Yi, Z.; Ni, W.; Zhang, Q.; Li, M. M.; Kan, B.; Wan, X. J.; Chen, Y. S. *J. Mater. Chem. C* **2014**, *2*, 7247.
- [50] Yang, X. N.; Loos, J.; Veenstra, S. C.; Verhees, W. J. H.; Wienk, M. M.; Kroon, J. M.; Michels, M. A. J.; Janssen, R. A. J. *Nano Lett.* **2005**, *5*, 579.
- [51] Peumans, P.; Yakimov, A.; Forrest, S. R. *J. Appl. Phys.* **2003**, *93*, 3693.

(Zhao, C.)